SCIENCE AND TECHNOLOGY ORGANIZATION
CENTRE FOR MARITIME RESEARCH AND EXPERIMENTATION

Reprint Series **CMRE-PR-2019-059**

Micro-bathymetry data acquisition for 3D reconstruction of objects on the sea floor

Diogo Machado, Thomas Furfaro, Samantha Dugelay

June 2019

Originally published in:

OCEANS 2017 - Aberdeen, UK, 19-22 June 2017,
doi: 10.1109/OCEANSE.2017.8084735

About CMRE

The Centre for Maritime Research and Experimentation (CMRE) is a world-class NATO scientific research and experimentation facility located in La Spezia, Italy.

The CMRE was established by the North Atlantic Council on 1 July 2012 as part of the NATO Science & Technology Organization. The CMRE and its predecessors have served NATO for over 50 years as the SACLANT Anti-Submarine Warfare Centre, SACLANT Undersea Research Centre, NATO Undersea Research Centre (NURC) and now as part of the Science & Technology Organization.

CMRE conducts state-of-the-art scientific research and experimentation ranging from concept development to prototype demonstration in an operational environment and has produced leaders in ocean science, modelling and simulation, acoustics and other disciplines, as well as producing critical results and understanding that have been built into the operational concepts of NATO and the nations.

CMRE conducts hands-on scientific and engineering research for the direct benefit of its NATO Customers. It operates two research vessels that enable science and technology solutions to be explored and exploited at sea. The largest of these vessels, the NRV Alliance, is a global class vessel that is acoustically extremely quiet.

CMRE is a leading example of enabling nations to work more effectively and efficiently together by prioritizing national needs, focusing on research and technology challenges, both in and out of the maritime environment, through the collective Power of its world-class scientists, engineers, and specialized laboratories in collaboration with the many partners in and out of the scientific domain.

NOTE: The CMRE Reprint series reprints papers and articles published by CMRE authors in the open literature as an effort to widely disseminate CMRE products. Users are encouraged to cite the original article where possible.

Micro-Bathymetry Data Acquisition for 3D Reconstruction of Objects on the Sea Floor

Diogo Machado*, Thomas Furfaro*, Samantha Dugelay*
*NATO Science and Technology Organization (STO), Centre for Maritime Research and Experimentation,
Viale San Bartolomeo 400, 19126 La Spezia, Italy
{Diogo.Machado, Thomas.Furfaro, Samantha.Dugelay}@cmre.nato.int

***Abstract*—This paper describes an effort to capture micro-bathymetry data for the end purpose of 3D object reconstruction, using an AUV-borne multibeam echo sounder. Due to the combination of relatively narrow across-track coverage and the navigation error of the vehicle, there is little guarantee that a single-pass scan will capture the target fully. A mission planning approach will be presented, with the goal of balancing mission duration and coverage. This method was demonstrated during a sea campaign in 2016 where multiple views of targets laying on the sea floor were acquired with the goal of developing a Target Registration System.**

I. Introduction

Underwater 3D reconstruction has been achieved by the use of optical[1],[2], acoustic [3] or both sensors [4]. The performance of the latter category is highly dependant on environmental characteristics that vary considerably, such as ambient light, light attenuation, and turbidity of the water.

Acoustic-based systems are more robust to these factors. Sonar systems, such as Side-Scan Sonar (SSS), Synthetic Aperture Sonar (SAS) and multibeam Sonars have been used to measure the texture of the sea floor. 3D reconstruction with imaging sonar systems can be achieved by using image features, combined with trajectory and kinematic information such as in [3], [5] and [6]. Sonar ranging systems are available from simple single beam systems to highly evolved systems with multiple beams (multibeam sonars) capable of simultaneously sampling hundreds of measurements from a section of the sea floor [7]. Multibeam profiling sonars have drastically reduced the time, hence cost, associated with bathymetric surveys.

Several motivations exist for reconstructing representations of underwater objects and structures. In environmental monitoring and geological surveying, 3D reconstruction is a research and monitoring tool. Although, in these settings, optical systems can present an important benefit with respect to sonar systems as color is often an attribute of significant interest [2].

Within the oil and gas industry and civil engineering fields, 3D reconstruction provides a tool for surveying, inspection and monitoring [8]. The structures of interest in these cases include infrastructure, such as bridges and dams, and the underwater equipment associated with oil and gas production, respectively.

The search for, and identification and monitoring of, underwater unexploded ordnance (UXO) [1] presents a long lasting challenge as navies and civil institutions struggle to find economical ways to appropriately mitigate risk to property and life. In these settings high resolution systems are required as the objects of interest are typically small, on the order of 1 meter.

Relatedly, mine countermeasure (MCM) activities are increasingly moving towards the use of high resolution acoustic sensors to classify mine-like objects (MLOs), particularly in situations where optical systems perform poorly.

The purpose of this work is to address this last group of applications, the identification of UXO or MLO, using a sonar system capable of sampling the sea bottom with high resolution. A multi-beam echosounder was mounted on an Autonomous Underwater Vehicle (AUV), to collect micro-bathymetry data, with a focusing on capturing multi-aspect data over man-made targets.

This paper presents a synopsis of the sampling challenge with potential mitigating solutions, as well as a preliminary analysis of the micro-bathymetry data gathered in the aforementioned experimental campaigns.

II. Platform

This work focuses on a short-range narrow beam multi-beam echo-sounder mounted on an AUV, with the eventual goal of performing *in situ* reacquisition and identification.

A. AUV

The AUV-of-opportunity for this effort is the REMUS 100, a common platform targeted largely at operational military users [9], while also providing other features that make it a good research platform. The basic vehicle model attempts to address the difficulties of underwater navigation through the use of a simple Long Baseline (LBL) transponder system [10] that is designed to bound the drift in navigation estimation error. This LBL system, as well as a Doppler Velocity Log (DVL), a Global Positioning System (GPS) receiver, a compass and a gyroscope, compose the total navigation suite.

The AUV also has a Conductivity Temperature and Depth (CTD) sensor, an Acoustic Doppler Current Profiler sensor (ADCP) as part of the DVL package, a dual frequency side-scan sonar (900/1800 kHz Marine Sonics Technology model SSPC) and an acoustic modem.

The adopted system architecture follows the *backseat-frontseat* philosophy that is commonly found on autonomous research platforms, as described in [11].

The AUV frontseat is in charge of all low level vehicle guidance, navigation, control and safety features, as well as some basic sensor management. The navigation information and vehicle status are both logged locally and made available in real-time via the REMUS REmote CONtrol protocol (RECON, [12]). The frontseat is a manufacturer provided-and-maintained unit that is closed to direct modification, but instead provides a command interface over which to send cues regarding vehicle navigation (i.e. driving), sensor configuration, or mission execution. The frontseat navigation estimate, as reported in the RECON protocol, suffers from quantization noise in both the position and time axes (Figure 9), with resolutions that are relatively coarse (state updates at 9 Hz, with 0.1s of precision in timestamping and 0.0001 minutes of precision in latitude/longitude).

Additional error may also be introduced by the operational limitations of the LBL transponder system. This is largely dictated by the relative movements of the LBL transponders in the water column due to wind, waves and current, and to deployment position accuracy.

B. MBES

The multi-beam echo sounder used in this work is the BlueView MB2250-N. The MBES has 256 beams, each 1 degree wide and separated by 0.18 degrees, filling a sector of 42°. The operational range is between 1 and 10 meters, and the acquisition rate, depending on the actual altitude, falls between 40-60 Hz. In practice, this creates a very narrow swath width at the operational altitude, requiring relatively direct fly-over to capture targets in view.

C. Backseat

The backseat controller and data recorder are composed by an industrial grade embedded computer, running Ubuntu 16.04 with the Robot Operating System (ROS) middleware. The computer is a SECO pITX-GX with a AMD GX-210GA, Dual Core @1.65GHz, 8GB RAM, 2 Gigabit Ethernet ports and a RadeonHD (GX-420CA) Graphics Processing Unit (GPU). The backseat logs sensor data and frontseat state information and also manages the configuration of the MBES sonar. The basic architecture is depicted in Figure 1.

The MBES interface driver relies on the manufacturers provided software development kit, which manages the Ethernet connection to the sonar hardware. The driver feeds the ROS environment with live sonar data and also saves it in a manufacturer-native format. The driver is multi-threaded, with individual threads responsible for:

1) Acquiring pings from the sonar and putting them into a thread safe queue;
2) Moving pings from the queue and saving them into the manufacturer-specific data file ;
3) Application management and synthesis of sonar data into ROS messages, including image and laser-scan-like (range and intensity vs. direction) messages.

A vehicle interface driver parses RECON data (received as UDP datagrams) and translates this to the ROS environment.

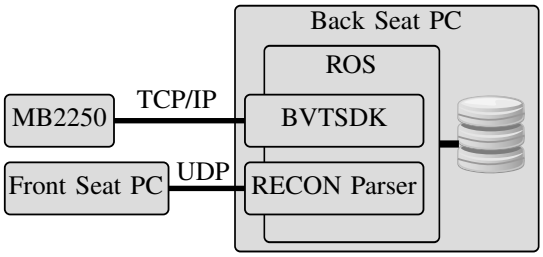

Fig. 1. MBES acquisition system.

These data also include the state estimate from the frontseat, which is used to transform the ping data from the sensor frame into the local reference frame.

III. Data Acquisition

The experiments described in this work were conducted by the NATO STO Centre for Maritime Research and Experimentation during the ONMEX'16 and MANEX'16 sea trials that occurred off the coasts of Toulon, France in September 2016 and Framura, Italy in October 2016 respectively.

A. Logistical Approach

During the at-sea experiments, target where deployed from the NRV *Alliance* research vessel with approximate locations known *a priori*. These target locations themselves have some error with respect to the absolute global frame. Additionally, because of the operational paradigm of LBL positioning systems, there can be inconsistencies between the true global reference frame and the frame that is measured underwater by the LBL system. For example, if there is some translational difference in the true versus planned transponder locations, this manifests as an inconsistency between the global and 'LBL frame'.

For this reason, we first relocalise targets in the local LBL frame by performing large, broad survey patterns, collecting side-scan sonar data. The side-scan contacts are then used as updated position estimates in the local frame. Currently this processing happens offline after the vehicle is recovered. The new contact positions are then used to program reacquisition missions that include multiple passes at multiple view directions, with approach geometries that specifically favor the MBES swath.

B. MBES Reacquisition Pattern

The specific trajectory shape (pattern) used during MBES reacquisition has been designed to mitigate the platform transience and increase the chance of a target view, while decreasing the survey time and area footprint. In particular, the REMUS100 equipped with the MBES has a significant transient in the yaw direction, which is exacerbated by very tight turns (e.g. 180 degrees), seen at point C of Figure 2. This could be accomodated by very long lead-in segments to guarantee that the vehicle reaches steady-state over the target area (point T in Figure 2). We have instead attempted to remove or at least minimize the number of overly acute

turns, adding transit segments between survey legs that run perpendicular to the target area (e.g. point A in Figure 2).

Additionally, there is an added challenge in capturing views on target due to the relative inaccuracy of the navigation system when compared to the multi-beam swath width. For this reason, we add multiple survey legs (Figure 2B) over the target in the same direction, with inter-leg spacing that provides some overlap (usually 1/3 of the swath width).

Lastly, because we are interested in multiple viewing angles, we include several survey-leg-sets over the target area in different directions. Figure 2 shows an example mission, with three viewing angles spaced evenly apart, with each direction having 3 legs that are spaced 1 meter apart.

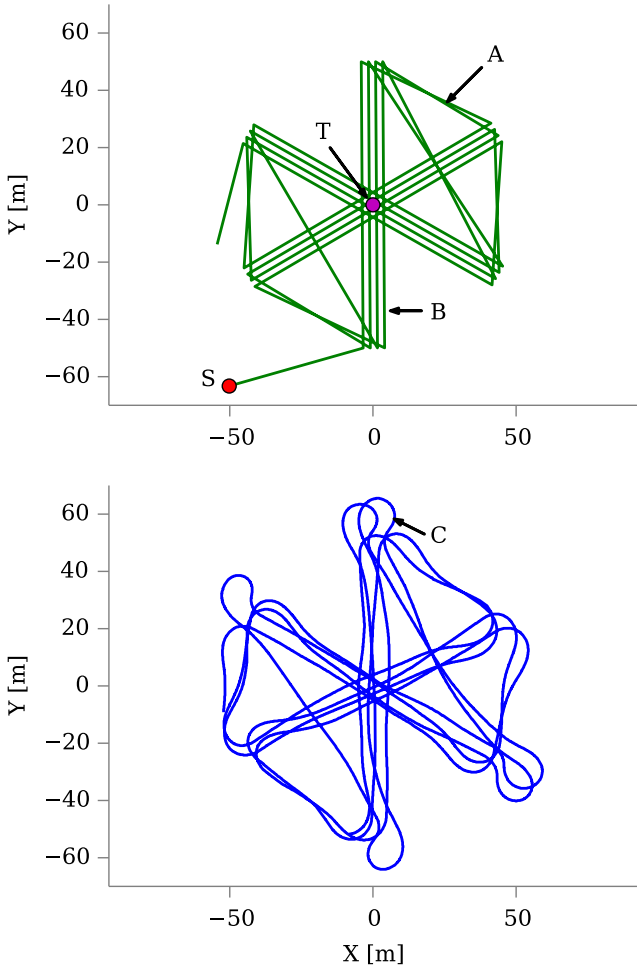

Fig. 2. Mission vs logged mission centred on theoretical target position.

During the subject sea trials, missions were run at 2, 4 and 6 meters altitude, which, with the MBES across track aperature of 42°, leads to swath widths of 1.5, 3.1 and 4.6 meters, respectively. Depending on this altitude, we obtained an along track resolutions between 25-40 mm as the distributions depicted in Figure 3 show.

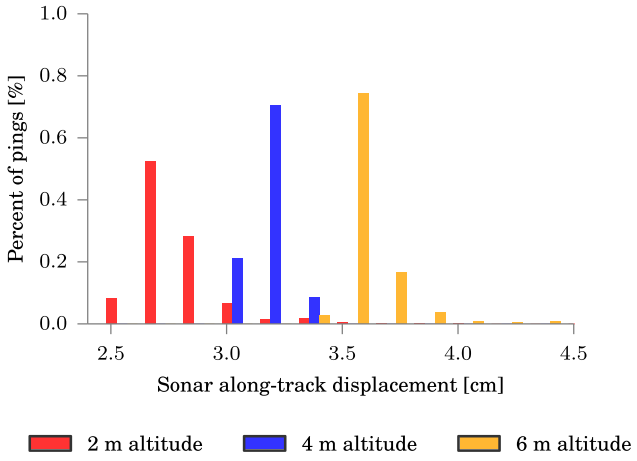

Fig. 3. Distribution of along-track ping displacement at 2, 4 and 6 meters altitudes.

C. Data Logging

MBES relevant data is saved in two distinct formats: (1) ROS 'bag' files, where telemetry (as reported by the front-seat) and segmented MBES pings are saved, and (2) Blueview 'son' files where all acquired pings are stored in their entirety. The bag file format is useful for playing back data in a time-synchronised manner, while the son file preserves more data about the pings themselves.

IV. Ping Segmentation and Point Cloud Construction

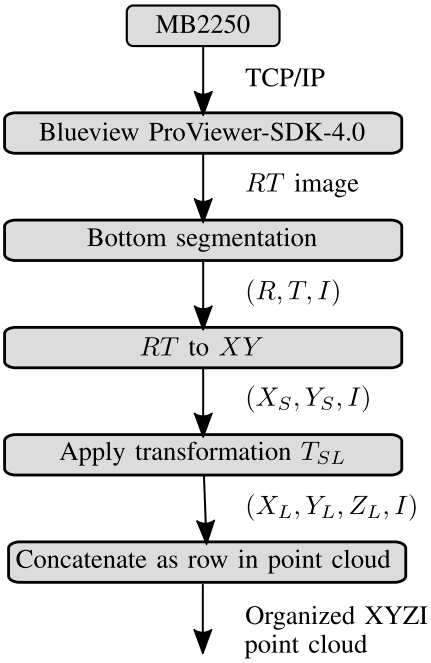

Fig. 4. Segmentation and point cloud construction steps.

Figure 4 shows the steps used to process raw sonar data into a 3D point cloud in a local reference frame.

Pings are accessed both in real-time and in post-processing using the manufacturer SDK (Software Development Kit). The pings are presented as 2D range-theta (RT) images, where each row represents a range or time delay and each column represents a sonar beam or Direction of Arrival (DOA). The value of a given pixel is the returned intensity for a given range and DOA. An example of such an image is depicted in Figure 5.

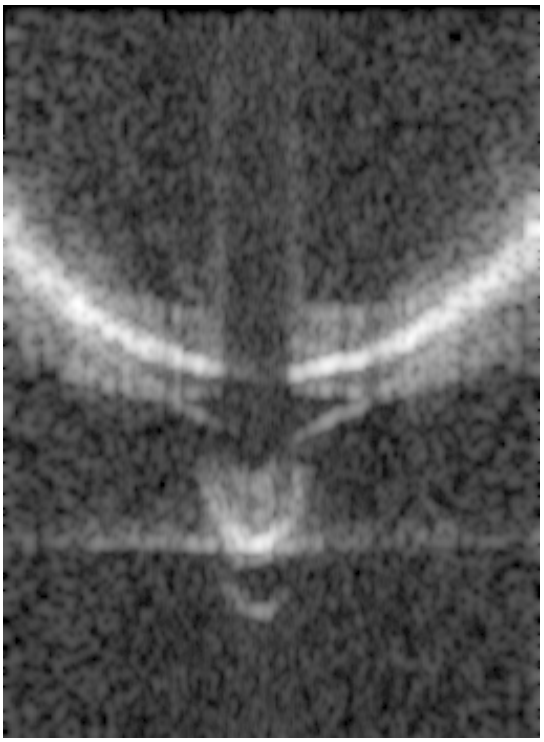

Fig. 5. Example of a single ping image when the AUV is passing over a cylindrical shape. Each row in the image represents a range (ρ) where top of the image are the furthermost ranges. Each of the columns represents a DOA (θ).

We have experimented with different surface detection approaches to segment the raw sonar ping into surface information. The most relevant algorithms were Weighted Mean Time (WMT) [13], Bearing Direction Indicator (BDI) [13] [14] and maximum intensities along each Direction of Arrival (DOA). BDI points have not been subject to the compression step as described in [14].

Figure 6 depicts a ping converted to Cartesian coordinates with the segmented points from the detection techniques overlaid. The BDI method was implemented without the data compression step as proposed in [14]. The Beam Maximum method was implemented on a ping image that was previously smoothed using a Gaussian kernel.

The time-slice based BDI technique is intended to be only used on beams grazing the surface with a low angle. Our idea when testing this method the idea was to check its effectiveness on outer beams or near vertical surfaces (e.g. sides of truncated cones) . Had it proved effective with our data, we could then combine it with another method more effective on beams hitting the surface with an higher angle.

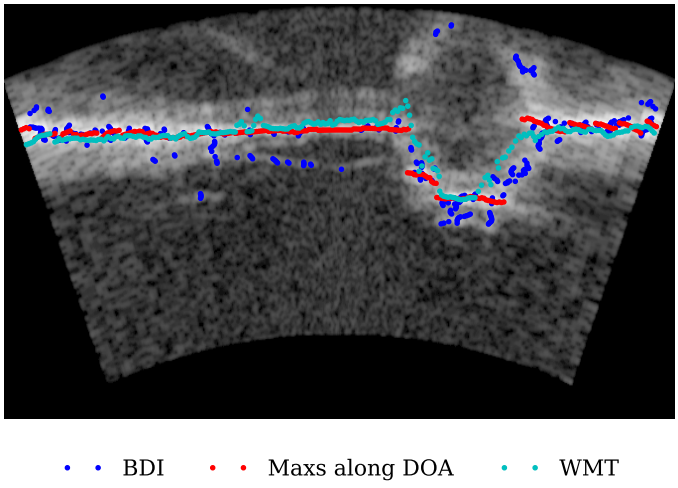

Fig. 6. Single ping of truncated cone object (trapezoidal cross-section). Ping has been transformed into Cartesian coordinates, with the origin (sonar head) located in the center bellow the image. Various bottom-detection techniques are overlaid.

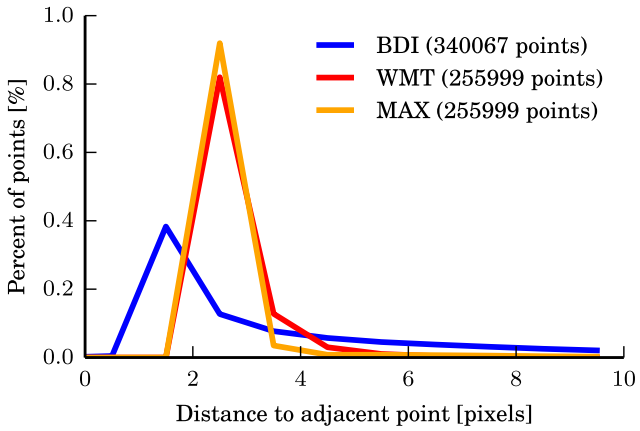

Fig. 7. Distribution of absolute distance to adjacent pixel.

Looking at Figure 6 it is apparent that the BDI method is noisier than the other methods. Figure 7 assists in this evaluation by showing that there are more BDI retrieved points with a larger absolute distance to adjacent points. Figure 6 shows that the BDI method is noisier than the other methods when segmenting the bottom surface. This observation was visually confirmed in several other images with different targets. In our case the other methods where therefore preferable for bottom segmentation.

Using WMT, although less noisy than BDI, it is observable in Figure 6 that the resulting points using this method did not trace the target with the same fidelity as when using the beam maximum on a smoothed ping image. This lack of fidelity is

specially evident on the areas around the target edges, where the returned energy is more dispersed along the beam.

Secondary echoes from target ensonification are also likely to contribute to this lack of shape fidelity.

The selected method consisted of firstly smoothing the RT image using a 5x5 Gaussian kernel and then segmenting using maximum intensities along each Direction of Arrival (DOA). The kernel size took into consideration that the beams are $1^\circ \times 1^\circ$ wide and their center is spaced by 0.18°.

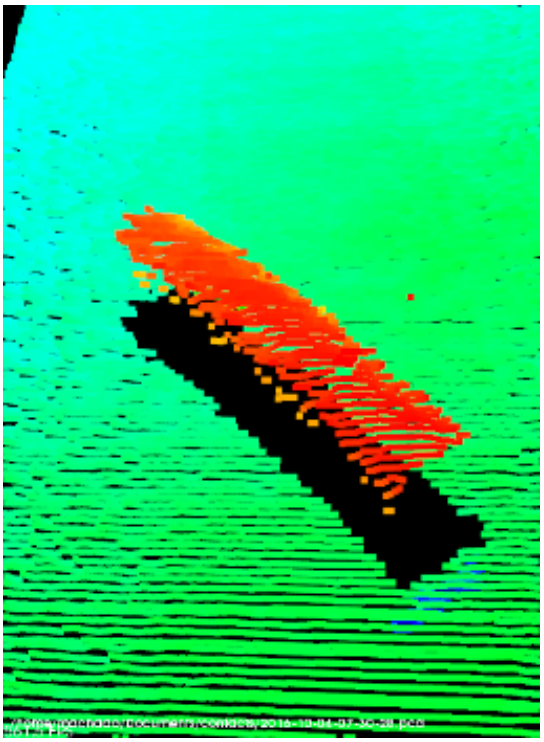

Fig. 8. 3D point cloud built using several segmented pings and adding the transformations from the sensor reference frame into the vehicle reference frame.

Following step in Figure 4 is the conversion from image coordinates into a Cartesian reference frame centred on the sonar head. Segmented ranges along each of the sonar DOA in the image (ρ_I, θ_I) are then converted from pixels to meters and degrees in the sensor reference frame (ρ_S, θ_S). For this step, the ping view from the sonar interface provides origin row ρ_{I0} (representing the sonar head), range resolution (η_R) and bearing resolution (η_T).

In Figure 5, the origin row ρ_0 (sonar head) is a row below the image and the first row represents the furthermost range. The conversion of the ranges is calculated via:

$$\rho_S = \eta_R(\rho_0 - \rho_I)$$

Given that θ_I is simply $[0, 1, 2, \ldots, n-1]$, where n is the total number of columns in the image, θ_S can be calculated with:

$$\theta_S = \eta_T \left(\theta_I - \frac{n}{2}\right).$$

Segmented points (ρ_S, θ_S) can then be converted to Cartesian coordinates (X_S, Y_S, Z_S) in the sensor frame with:

$$\begin{bmatrix} X_S \\ Y_S \\ Z_S \end{bmatrix} = \begin{bmatrix} \rho_S sin(\theta_S) \\ \rho_S cos(\theta_S) \\ 0 \end{bmatrix}.$$

In order to reconstruct a local map, points in the sonar reference frame have to be transformed to the local reference frame by T_{SL},

$$T_{SL} = T_{BL} T_{SB},$$

where T_{SB} is the transformation matrix from the sensor reference frame to the body reference frame and T_{BL} is the transformation matrix from the body to the local reference frame. T_{SL} is computed for every ping using the vehicle estimated pose and position.

To mitigate sudden pose changes caused by measurement and time quantization errors, we applied an Extended Kalman Filter (EKF) to smooth these quantities. Those errors and the EKF correction are shown in Figure 9. T_{BL} is composed using these filtered measurements for each ping, where the pose is interpolated based on the timestamp of ping itself.

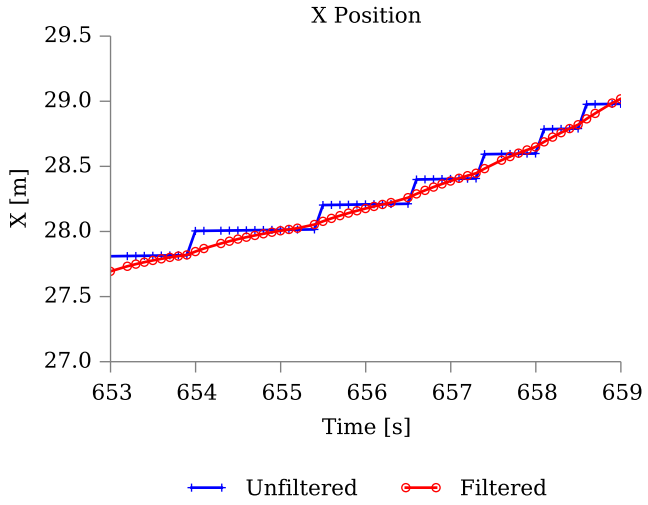

Fig. 9. Comparison between raw and filtered x position measurements.

Ping data from the Cartesian coordinates in the sensor frame are transformed into the local frame via:

$$\begin{bmatrix} X_L \\ Y_L \\ Z_L \end{bmatrix} = T_{SL} \begin{bmatrix} X_S \\ Y_S \\ Z_S \end{bmatrix}$$

Local points from the same ping are added as a row to an organized point cloud [15]. By keeping the cloud organized we maintain the relationship with adjacent points. Figure 10 shows an example of a patch from a height map built from an organized point cloud. Object in the image is a 40 cm high truncated cone. White pixels next to object edges are pixels

which we set to not-a-number (NaN) because their intensities was lower than a set threshold. This threshold is useful to remove outliers created by pixels with a low intensity. The Z height-map along with the other maps (X, Y and Intensities) are practical when we want to use image and/or matrices processing techniques and libraries (i.g.:opencv,matlab/octave) to process the data efficiently.

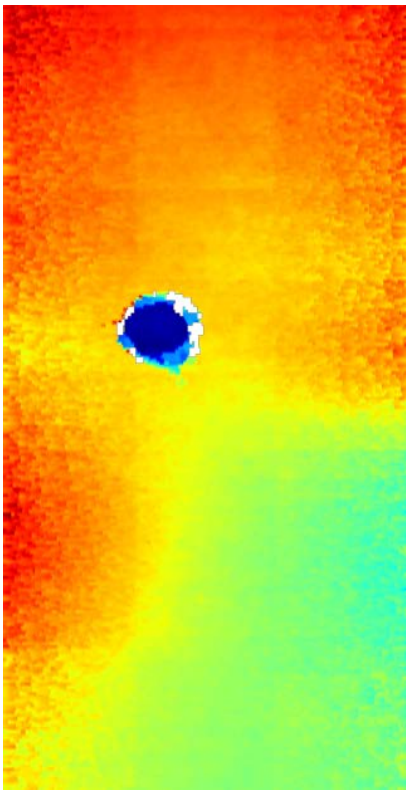

Fig. 10. Patch from height map built from organized point cloud. Each row on the figure represents a single ping and each column is a DOA. Each pixel colour has been mapped to a magnitude of the Z coordinate on a local reference frame.

Figure 11 illustrates a close up of the processed data collected while performing the pattern described in Figure 2. Three distinct transits within the mission where the same object was ensonified. The wedge shape object is about 1 meter long and, in this case, the combined navigation error manifests as a roughly 4 meter inconsistency between different views within the same mission.

V. Conclusion and Future Work

This paper describes the data acquisition and initial segmentation strategy for using micro-bathymetry data to perform 3D reconstruction.

Segmentation strategies for estimating reflecting surfaces from ping data were explored. In order to mitigate quantizations errors in pose information, an Extended Kalman Filter was used to filter the system state readings.

An interesting future experiment would be to mount the MBES with some inclination, as opposed to the current vertical mounting position allowing a richer set of features from targets

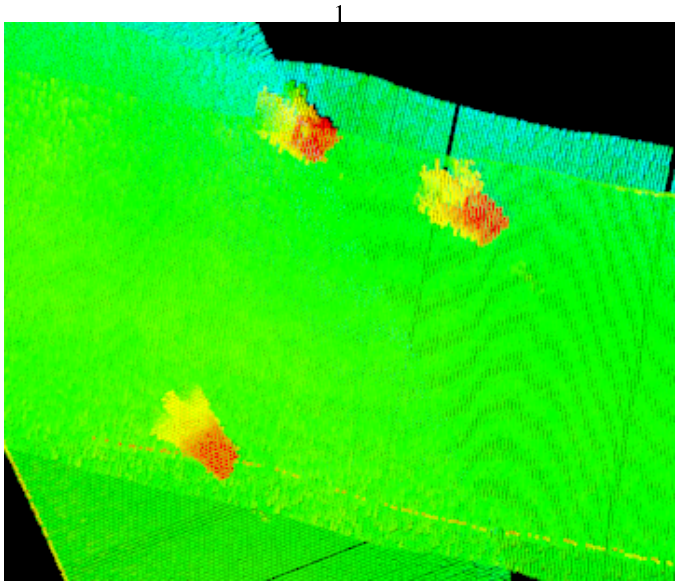

Fig. 11. Multiple views of an approximately 1 meter long wedge-shaped object on the sea bottom. Due to the navigation error the object is depicted at different positions on each of the tracks.

with near vertical sides. We have prepared a larger vehicle to mount this sensor with different inclinations and intend to experiment on acquiring data with different inclinations.

The data acquired has multiple contacts of different types in different environmental conditions.

This data can now be used in scientific work in areas like clustering, registration, automatic detection/classification/identification. Furthermore, the highly descriptive data could also be used to build a map and feed a localization framework with robust landmarks.

References

[1] A. Shihavuddin, N. Gracias, R. Garcia, R. Campos, A. C. Gleason, and B. Gintert, "Automated Detection of Underwater Military Munitions Using Fusion of 2D and 2.5D Features From Optical Imagery," *Marine Technology Society Journal*, vol. 48, no. 4, pp. 61–71, jul 2014. [Online]. Available: http://openurl.ingenta.com/content/xref?genre=article{\&}issn=0025-3324{\&}volume=48{\&}issue=4{\&}spage=61

[2] C. Beall, B. J. Lawrence, V. Ila, and F. Dellaert, "3D reconstruction of underwater structures," in *2010 IEEE/RSJ International Conference on Intelligent Robots and Systems*. IEEE, oct 2010, pp. 4418–4423. [Online]. Available: http://ieeexplore.ieee.org/document/5649213/

[3] M. Babaee and S. Negahdaripour, "3-D object modeling from occluding contours in opti-acoustic stereo images," *Oceans - San Diego, 2013*, pp. 1–8, 2013.

[4] G. Inglis, "Hybrid Optical Acoustic Seafloor Mapping," Ph.D. dissertation, 2013. [Online]. Available: http://digitalcommons.uri.edu/oa{_}diss/64

[5] N. Brahim, D. Guériot, S. Daniel, and B. Solaiman, "3D reconstruction of underwater scenes using DIDSON acoustic sonar image sequences through evolutionary algorithms," in *OCEANS 2011 IEEE - Spain*, 2011.

[6] E. Coiras, Y. Petillot, and D. M. Lane, "Multiresolution 3-D Reconstruction From Side-Scan Sonar Images," *IEEE Transactions on Image Processing*, vol. 16, no. 2, pp. 382–390, feb 2007. [Online]. Available: http://ieeexplore.ieee.org/document/4060928/

[7] D. A. Yakubovskiy, "Navigation Sonar for the Ship Operator: Forward Looking Sonars and Multibeam Echosounders Explained," 2010. [Online]. Available: http:

//www.farsounder.com/files/NavigationSonarForTheShipOperator{_}ForwardLookingSonarsAndMultibeamEchosoundersExplained.pdf

[8] J. C. Leedekerken, M. F. Fallon, and J. J. Leonard, "Mapping complex marine environments with autonomous surface craft," in *Springer Tracts in Advanced Robotics*, vol. 79, 2014, pp. 525–539.

[9] C. von Alt, B. Allen, T. Austin, and R. Stokey, "Remote environmental measuring units," in *Proceedings of IEEE Symposium on Autonomous Underwater Vehicle Technology (AUV'94)*. IEEE, 1995, pp. 13–19. [Online]. Available: http://ieeexplore.ieee.org/document/518601/

[10] L. Freitag, M. Grund, S. Singh, J. Partan, P. Koski, and K. Ball, "The WHOI Micro-Modem: An acoustic communications and navigation system for multiple platforms," in *Proceedings of MTS/IEEE OCEANS, 2005*, vol. 2005, 2005.

[11] D. P. Eickstedt and S. R. Sideleau, "The Backseat Control Architecture for Autonomous Robotic Vehicles: A Case Study with the Iver2 AUV," *Marine Technology Society Journal*, vol. 44, no. 4, pp. 42–54, 2010. [Online]. Available: http://openurl.ingenta.com/content/xref?genre=article{\&}issn=0025-3324{\&}volume=44{\&}issue=4{\&}spage=42

[12] Maritime Kongsberg, "REMUS REmote CONtrol PROTOCOL KMHYD-Man-0002," 2012.

[13] C. Moustier, "Signal Processing for Swath Bathymetry and Concurrent Seafloor Acoustic Imaging," in *Acoustic Signal Processing for Ocean Exploration*. Dordrecht: Springer Netherlands, 1993, pp. 329–354. [Online]. Available: http://link.springer.com/index/10.1007/978-94-011-1604-6{_}33

[14] D. L. d. S. Pereira and John E. Hughes Clarke, "Improving shallow water multibeam target detection at low grazing angles:," in *US Hydrographic Conference*, 2015.

[15] Pointclouds.org, "The PCD (Point Cloud Data) file format." [Online]. Available: http://pointclouds.org/documentation/tutorials/pcd{_}file{_}format.php

Document Data Sheet

Security Classification		Project No.
Document Serial No.	**Date of Issue**	**Total Pages**
CMRE-PR-2019-059	June 2019	7 pp.

Author(s)

Diogo Machado, Thomas Furfaro, Samantha Dugelay

Title

Micro-bathymetry data acquisition for 3D reconstruction of objects on the sea floor

Abstract

This paper describes an effort to capture micro-bathymetry data for the end purpose of 3D object reconstruction, using an AUV-borne multibeam echo sounder. Due to the combination of relatively narrow across-track coverage and the navigation error of the vehicle, there is little guarantee that a single-pass scan will capture the target fully. A mission planning approach will be presented, with the goal of balancing mission duration and coverage. This method was demonstrated during a sea campaign in 2016 where multiple views of targets laying on the sea floor were acquired with the goal of developing a Target Registration System.

Keywords

Three-dimensional displays, navigation, sensors, sonar measurements, synthetic aperture sonar, image segmentation

Issuing Organization

NATO Science and Technology Organization
Centre for Maritime Research and Experimentation

Viale San Bartolomeo 400, 19126 La Spezia, Italy

[From N. America:
STO CMRE
Unit 31318, Box 19, APO AE 09613-1318]

Tel: +39 0187 527 361
Fax:+39 0187 527 700

E-mail: library@cmre.nato.int